Inorg. Chem. **2002**, *41*, 856–863

Optical Investigations of Alkali Metal Thiomanganates(II) Containing Isolated Complexes as Well as Chain and Planar Compounds

Ulrike Rosellen and Hans-Herbert Schmidtke*

Institut für Theoretische Chemie, Heinrich-Heine-Universität, D-40225 Düsseldorf, Germany

Received March 26, 2001

Tetracoordinated Mn(II) complexes providing different molecular structures were investigated using various spectroscopical procedures. Na_6MnS_4 contains separate pseudotetrahedral Mn–S complex units, K_2MnS_2 has chains of edge-shared tetrahedra, and $Cs_2Mn_3S_4$ crystallizes in corresponding layers. Also doped materials, i.e., $Cs_2(Mn_xZn_{1-x})_3S_4$ with $0.0 < x < 1.0$, are considered. Absorption spectra recorded from samples incorporated in polyethylene pellets and excitation spectra taken from pure materials at 15–20 K temperature are assigned on the basis of energy level calculations obtained from the angular overlap model. All compounds exhibit intensive emission in the red, some of them also in the yellow region, which both are investigated in the temperature range from 12.5 to 250 K, in some cases varying the excitation power and excitation wavelength. Decay measurements supply lifetimes and activation energies evaluated from Arrhenius plots. The results support an assignment of both types of emissions to MnS_4 complex entities for all compounds, the red emission from the lowest excited level (Kasha luminescence) and the yellow emission, observed for some of the compounds with increasing intensity at lower temperature, from higher electronic levels.

1. Introduction

Due to the particular magnetic and optical properties of Mn^{2+} doped in ZnS, it was the subject of numerous publications in the past decades.[1−8] The present ternary alkali−thiomanganates now offer the opportunity to investigate also chemical compounds of different molecular structure starting from isolated mononuclear Mn complexes leading to two-dimensional layer structures.

It is generally agreed upon that the 18000−26000 cm^{-1} bands in the absorption and emission spectrum of the primarily investigated ZnS:Mn are assigned to ligand field transitions of tetrahedrally coordinated Mn^{2+} ions (d^5).[2,6,8,9] Agreement seems to be obtained as well on the explanation of the yellow emission at 17000 cm^{-1} which is assigned to the $^4T_1(G) \rightarrow {}^6A_1(S)$ d−d transition of this chromophore.[4,9,10] The origin of the red luminescence at about 15000 cm^{-1} observed in systems with concentrations larger than ca. 1 mol % Mn^{2+} in ZnS is, however, has been explained contradictorily. While earlier it has been attributed to Mn pairs and clusters,[3,11] which was concluded also from absorption spectra of high resolution,[1] some later authors preferred an assignment to energy transfer processes between excited Mn ions and unknown red emitting centers.[4,5,12,13] Possible suggestions attributing the red emission to octahedrally coordinated Mn impurifications must be excluded because Stokes shifts (calculated from about 16700 cm^{-1} absorption [1,10,14,15] and 15000 cm^{-1} emission maxima for this interpretation) are expected to be larger than for the tetrahedral coordination (19000 → 17000 cm^{-1} yellow emission[2,6,8,10,15]) due to the higher ligand field and larger bond energy changes in case of the octahedron. Also emission from hexacoordinated Mn^{2+} of α-MnS (rocksalt

* Author to whom correspondence should be addressed. E-mail: schmidtke@theochem.uni-duesseldorf.de.

(1) McClure, D. S. *J. Chem. Phys.* **1963**, *39*, 2850.
(2) Gumlich, H.-E.; Pfrogner, R. L.; Schaffer, J. C.; Williams, F. E. *J. Chem. Phys.* **1966**, *44*, 3929.
(3) Gumlich, H.-E. *J. Lumin.* **1981**, *23*, 73.
(4) Dang Dinh Thong; Goede, O. *Phys. Status Solidi B* **1983**, *120*, K 145.
(5) Benoit, J.; Benolloul, P.; Geoffroy, A.; Balbo, N.; Barthou, C..; Denis, J. P.; Blanzat, B. *Phys. Status Solidi A* **1984**, *83*, 709.
(6) Goede, O.; Heimbrodt, W. *Phys. Status Solidi B* **1988**, *146*, 11.
(7) DeVisschere, P.; Neyts, K. *J. Lumin.* **1992**, *52*, 313.
(8) Boulanger, D.; Parrot, R.; Pohl, U. W.; Litzenburger, B.; Gumlich, H.-E. *Phys. Status Solidi B* **1999**, *213*, 79.
(9) Pohl, U. W.; Gumlich, H.-E. *Phys. Rev. B* **1989**, *40*, 1194.
(10) Borisenko, N. D.; Bulanyi, M. F.; Kodzhespirov, F. F.; Polezhaev, B. A. *J. Appl. Spectrosc.* **1992**, *55*, 911.
(11) Neumann, E. Doctorate Thesis D83, Technische Universität Berlin, 1971.
(12) Goede, O.; Dang Dinh Thong. *Phys. Status Solidi B* **1984**, *124*, 343.
(13) Katiyar, M.; Kitai, A. H. *J. Lumin.* **1990**, *46*, 227.
(14) Komura, H. J. *Phys. Soc. Jpn.* **1969**, *26*, 1446.
(15) Goede, O.; Heimbrodt, W.; Weinhold, V. *Phys. Status Solidi B* **1986**, *136*, K49.

10.1021/ic010333c CCC: $22.00
Published on Web 01/30/2002

structure) has been found[16] at 11530 cm^{-1}, which is significantly lower than the present red emissions. Investigations on present ternary manganese sulfide complexes do not support the preceding explanations; we shall rather favor assignments to transitions within the perturbed d shell of Mn as it has been considered as a possible choice already in an earlier work.[4]

The present compounds contain sulfur-coordinated Mn(II) tetrahedra which they have in common with the ZnS:Mn system. With lower concentrations of counter (alkali) ions the clustering of Mn units increases: while Na_6MnS_4 includes separated complex (pseudo)tetrahedra, the compounds with smaller contents of alkali metal ions, i.e., K_2MnS_2, have one-dimensional infinite chains, $^1_\infty[MnS_{4/2}]$, and $Cs_2Mn_3S_4$ crystals contain two-dimensional layers, $^2_\infty[Mn_3S_{16/4}]$.[17] From the layer compound, in addition, a continuous series of doped materials,[18] i.e., $Cs_2(Mn_xZn_{1-x})_3S_4$ with $0 < x < 1$, could be investigated. With this set of compounds an investigation of optical properties of ternary manganese sulfides depending on the structure and concentration has been carried out. A comparison with iron sulfides, also available as isolated complex units and extended chain molecules,[19] is of great interest. Although chemical bonding in Fe(III) sulfides is more covalent due to the higher metal charge, the low-energy absorption bands of these compounds could be assigned to d−d-transitions and were explained by angular overlap model (AOM) calculations. Since d electrons of present manganese compounds are expected to be more localized on the metal, the corresponding optical spectra should be due to ligand field transitions as well. This applies also for systems with extended molecular structures. Their emission spectra show, however, some specific differences, which will be the main subject of the present investigation.

2. Experimental Section

The compounds have been supplied by the Institute of Inorganic Chemistry of the Technical University in Aachen, Germany. Syntheses, structural properties, and magnetic properties are given in the literature.[18,20,21]

2.1. Sample Preparation. In particular Na_6MnS_4 and K_2MnS_2 are extremely sensitive to moisture from the air. For reliable measurements they must be handled in a glovebox filled with dried argon. The absorption spectra were recorded from KBr or polyethylene (PE) pellets. The PE samples proved to furnish better resolved spectra, for which possible reaction with the medium is avoided. In a typical preparation a microcrystalline sample of the compound is mixed in argon atmosphere with 2−20-fold excess of dried PE (spectroscopically pure quality) and filled in a 5 mm cavity of a press tool. The sample protected by a plastic bag is removed from the box through a lock chamber and pressed in this cover forming a disk by applying 2 t of pressure. Introduction into the cryostat carried out as fast as possible is followed by immediate evacuation. If the size of the cryostat is sufficiently small to be handled in the glovebox, the disk can be mounted without removal from the inert atmosphere.

For performing excitation and emission measurements, powder samples of pure crystals have been used filled in an aluminum holder in a glovebox of argon atmosphere. Since this cryostat could not be placed into the drybox, the sample carrier had to be shortly exposed to air atmosphere before the cryostat was evacuated. Protection by storing the sample in a glass tube, although when mounted by a heat conducting paste on the cooling finger, supplies only the red luminescence spectrum (about 15000 cm^{-1}, half-width 1800 cm^{-1}); the strongly temperature dependent yellow emission (17000 cm^{-1}) will not be detected. This observation obviously is due to insufficient cooling at the sample despite all precautions being undertaken.

Samples of $Cs_2(Mn_xZn_{1-x})_3S_4$ for all Mn contents x are less sensitive to moisture and can be shortly exposed to the atmosphere without further care.

2.2. Optical Investigations. The absorption spectra in the visible and near-UV region were recorded on a Cary 04 instrument of Varian which is equipped with a tungsten and a deuterium lamp. For low-temperature measurements the sample compartment had to be extended by constructing a lens system on a microoptical bank which allows light focusing on a helium LT-3-110C cryostat of Air Products mounted on an adjustable table. Since with this device the background absorption is not compensated by the parallel beam, the background radiation must be monitored separately for each recording of a spectrum. Spectral resolution obtained from this setup was in general about 2 nm, in some cases 0.5 nm. By heating against the cooling power, the temperature of the samples could be chosen between 15 and 300 K. Heating facilities and temperature control close to the sample mull were supplied by a Heli-Tran control panel model OC-20 of Air Products and Chemicals Company using a chromel/gold thermoelement.

For luminescence measurements an argon ion laser type 2016 of Spectra Physics (4 W power), from which the plasma lines are removed by a laser monochromator (type Laserspek III), was used as light source. Cooling between 12 and 300 K was provided by a closed-cycle system R 210 of Leybold-Heraeus where the temperature is controlled by a heating furnace Variotemp HR-1 of the same manufacturer. For temperature between 2 and 12 K a bath cryostat of CryoVac has been used equipped with two tank supplies for liquid nitrogen and helium, respectively.

A Jobin Yvon monochromator H 250 with lattices appropriate for different wavelength regions is used for measurements between 13 K and room temperature; a Czerny-Turner double monochromator from McPherson is applied when recording low-temperature spectra at 2 K.

Emission intensities were analyzed using primarily an optical multichannel analyzer (OMA) model 1460/1462 of EG&G which allows light detection of different wavelengths on 750 photodiodes. For decay measurements, a photomultiplier C31034 of RCA has been used which was equipped with a Peltier cooler TE 104 Rf of PRA for quenching thermal noise. Improved signal−noise relations were obtained by an amplifier model 1763 and an amplifier/discriminator 1762 both of PRA.

The excitation spectra were recorded from a device consisting of an XBO 150W Osram xenon lamp and a Jobin Yvon monochromator for selecting excitation light choosing wavelengths 290−600 nm in steps of 5 nm. The light intensity was controlled by an optical power meter 835 of Newport Corporation equipped with a

(16) Goede, O.; Heimbrodt, W.; Weinhold, V.; Schnürer, E.; Eberle, H. G. *Phys. Status Solidi B* **1987**, *143*, 511.
(17) Bronger, W.; Müller, P. *J. Alloys Compd.* **1997**, *246*, 27.
(18) Bronger, W.; Hendricks, U.; Müller, P. *Z. Anorg. Allg. Chem.* **1988**, *559*, 95.
(19) Packroff, R.; Schmidtke, H.-H. *Inorg. Chem.* **1993**, *32*, 654.
(20) Bronger, W.; Balk-Hardtdegen, H. *Z. Anorg. Allg. Chem.* **1989**, *574*, 89.
(21) Bronger, W.; Balk-Hardtdegen, H.; Schmitz, D. *Z. Anorg. Allg. Chem.* **1989**, *574*, 99.

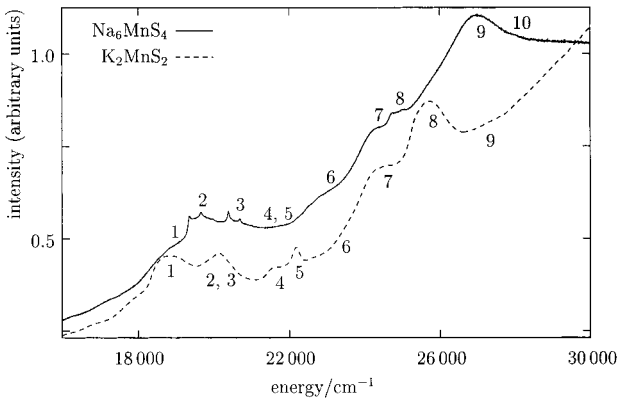

Figure 1. Absorption spectra of Na_6MnS_4 (18 K) and K_2MnS_2 in polyethylene pellets. Spectral resolution 0.5 and 2 nm, respectively. The numbers refer to the transitions resulting from the assignment of Table 1.

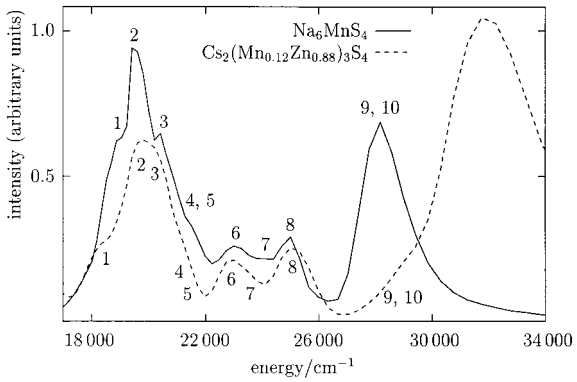

Figure 2. Excitation spectra of Na_6MnS_4 and $Cs_2(Mn_{0.12}Zn_{0.88})_3S_4$ crystal powders at 12 K detected from the red emission. Due to variation of wavelength in steps of 5 nm, the spectra contain some discontinuities.

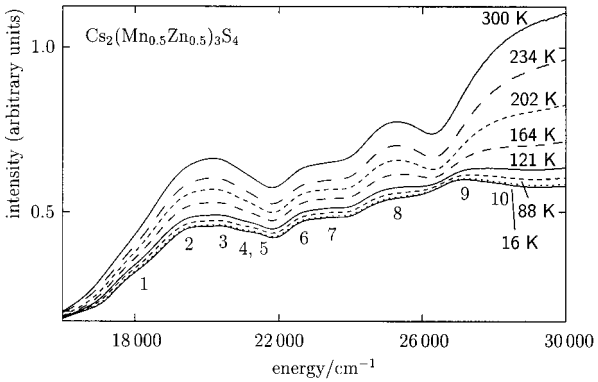

Figure 3. Absorption spectra of $Cs_2(Mn_{0.5}Zn_{0.5})_3S_4$ in polyethylene pellets recorded at different temperatures.

detector 818 UV and an attenuator 883 UV furnished by the same company. The emitted light was monitored by the OMA as used above.

For decay measurements the laser equipment from the luminescence measurements was used. The modulation of the laser signal was carried out by introducing an acousto-optical modulator EFC-C200-PH of Matsushita into the light beam which was controlled by signals of a pulse generator Turbo MCS T914 of EG&G Ortec. The trigger signal also controls a multichannel analyzer for which the above RCA photo multiplier is used equipped with an IBM-PC/AT of EG&G Ortec providing Turbo-MCS software. This arrangement allows the determination of life times using multichannel scaling (MCS) techniques. For more experimental details see ref 22.

3. Results

3.1. Absorption and Excitation Spectra. The absorption spectra of Na_6MnS_4 and K_2MnS_2 recorded from polyethylene pellets are illustrated in Figure 1. The observed bands and shoulders are located on a broad background absorption increasing toward higher frequencies resulting in relatively poor resolution that limits the accuracy of wavenumbers of band positions. This background is primarily due to scattering effects from the polyethylene pellets since it is absent when considering excitation spectra recorded from the red emission of microcrystalline samples of pure materials (Figure 2). In the region 19000−21000 cm^{-1} of Na_6MnS_4 in absorption a recording with higher sensitivity exhibits some vibrational fine structure.[22,23]

The absorption spectra of Mn doped in $Cs_2Zn_3S_4$ show a series of band shoulders located on a background absorption which become more distinct for higher Mn concentration.[22] A temperature dependent spectrum of a 50% doped sample is depicted in Figure 3. Spectra of all present compounds exhibit absorption peaks or inflections at very similar positions, indicating that d−d transitions are largely determined by local MnS_4 complex entities forming essentially the active chromophores in these materials. No additional bands can be detected which may be assigned to complex pairs or clusters. This might be due to the moderate quality of resolution obtained which obscures minor band splittings. The main band profiles are, however, determined by the MnS_4 level system. Some presumably antiferromagnetic coupling can be detected from increased band intensities measured at higher temperature (cf. Figure 3) which arise from larger occupations of excited pair states giving rise to spin-allowed transitions.

Peaks in excitation spectra of the layer compounds, $Cs_2(Mn_xZn_{1-x})_3S_4$, are much better resolved for higher Mn concentrations.[22] The band close to 32000 cm^{-1} is due to the zinc host lattice; it gradually loses intensity relative to the d−d bands when increasing the Mn content.

Since apparently all present spectra result from MnS_4 chromophores which are somewhat distorted from tetrahedral coordination due to different site symmetry in the crystals, we can apply AOM calculations on the mononuclear species using the valence angles obtained from crystal structure investigations.[17,18,20,21] For Na_6MnS_4 containing separate Mn complexes of C_{3v} local symmetry, the results are given in Table 1. The tetrahedral band assignments agree with corresponding results reported for ZnS:Mn from Gumlich and co-workers[2] and with investigations on bis(tetraphenyldithioimidodiphosphinato)Mn(II) of Siiman and Gray[24] which contain tetracoordinated sulfur chromophores as well. Identical assignments of corresponding bands in all spectra considered are indicated by equal peak numbering in the

(22) Rosellen, U. Doctorate Thesis, Heinrich-Heine-Universität Düsseldorf, 1996.
(23) Rosellen, U.; Schmidtke, H.-H. To be published.
(24) Siiman, O.; Gray, H. B. *Inorg. Chem.* **1974**, *13*, 1185.

Table 1. Band Assignments and Optimized AOM Results for a Trigonally Distorted MnS_4 Chromophore Calculated from the Parameters (in cm^{-1}) $B = 519$, $C = 3200$, $\zeta = 0$ and $Dq = -454$ Using the Structural Data of Na_6MnS_4 (MnS_1 242.6 pm, MnS_3 242.4 pm, S_1MnS_3 108.17°, S_3MnS_3 110.74°)[18]

transition			energy, cm^{-1}		
			measd[a]		
T_d $^6A_1(S) \rightarrow$	C_{3v} $^6A_1 \rightarrow$	band no.	abs	exc	calcd
$^4T_1(G)$	^4E	1	18830	18800	18614
	$^4A_2$				18780
$^4T_2(G)$	$^4A_1$	2	19750	19700	20359
	^4E	3	20650	20650	20382
$^4E(G)$	^4E	4	21450	21400	21188
$^4A_1(G)$	$^4A_1$	5	21450	21400	21190
$^4T_2(D)$	^4E	6	23100	23100	23886
	$^4A_1$	7	24200	24100	23997
$^4E(D)$	^4E	8	25000	25000	24821
$^4T_1(P)$	$^4A_2$	9	27100	28100	28011
	^4E	10	28050		28257

[a] Band centers from Na_6MnS_4 spectra.

figures. Band splittings in spectra of the chain and layer compounds are due to D_2 or C_2 site symmetry. Spin−orbit coupling giving rise to multiplet splittings of maximal 130 cm^{-1} (obtained from ligand field calculations[25] on $MnBr_4^{2-}$ with $\xi = 320$ cm^{-1}) has been neglected. The calculated model parameters obtained from the fit of the spectra agree with those expected from the spectrochemical and the nephelauxetic series which are known, respectively, for ligand field parameters Dq and Racah parameters B and C of transition metal complex compounds.[26] The low B parameter compares well with that of the Siiman and Gray compound.[24] This finding is explained from the strong covalency by which B parameters are decreased more than C as can be shown by analyzing the Slater−Condon parameters F_2 and F_4.[27] The degree of covalency in the metal−ligand bands reflected by the nephelauxetic ratio $B_{complex}/B_{free\ ion}$ that relates the electron repulsion parameters derived from the spectra of the complex compound and of the free ion is 0.54 for $Mn^{II}S_4$ and compares with 0.42 for $Fe^{III}S_4$.[19] The splitting due to lower symmetry is generally calculated smaller than observed in the experiment. This shortcoming is conveniently taken care of by introducing expansion coefficients for d orbitals providing different covalency effects in molecular orbitals of dfferent symmetry.[28]

3.2. Emission Spectra. All compounds of present interest show efficient luminescence in the red; Na_6MnS_4 and $Cs_2Zn_3S_4$ with low Mn concentration emit in the yellow region as well. This finding agrees with earlier concentration dependent investigations on the ZnS:Mn system.[3−6,12,29]

In Figure 4 the luminescence spectra are illustrated together with the temperature dependence of integral intensities of both emissions for the compounds indicated. At low

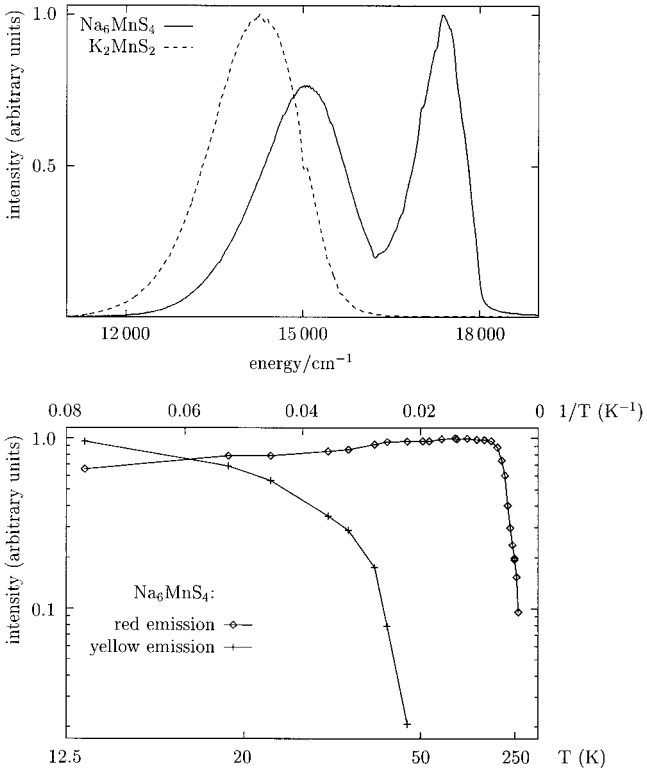

Figure 4. Emission spectra of Na_6MnS_4 and K_2MnS_2 from crystal powders at 13 K and temperature dependence of the integral intensity of the red and yellow emission bands of Na_6MnS_4 ($\lambda_{exc} = 488$ nm). Corrections for intensity changes of excitation light are neglected (see text).

temperature the yellow band is the main component of emission; it loses, however, intensity on temperature increase in favor of the red luminescence which is dominant at $T > 50$ *K*. Other than Na_6MnS_4, from K_2MnS_2 only red emission is observed with intensity decrease toward higher temperature, in particular from about 50 K on. Similar temperature behavior is known from ZnS:Mn.[4]

The temperature dependence of luminescence from $Cs_2(Mn_xZn_{1-x})_3S_4$ doped with Mn of different concentrations is presented in Figure 5. A correction for temperature dependent absorption (Figure 3) is only minute. The general course of the emission curves remains unchanged. Yellow luminescence is detected only from systems with low Mn concentrations ($x < 0.12$); emission bands in the red are observed from all compounds independent of concentration. The temperature dependent emission intensities are again closely related to those observed for the preceding compounds which contain isolated complexes or molecular chains (cf. Figure 4). The red emission gains intensity at the expense of the yellow emission (if observable) with increasing Mn concentration. A crossing of temperature curves for red and yellow emission intensity as shown in Figure 4 is also observed from the doped compounds with low Mn concentration ($x = 0.02$ or 0.05). The fine structure detected in the yellow emission is not well-resolved. Visual inspection of band components indicates peak intervals of 260−300 cm^{-1}, which is close to 250 cm^{-1} vibrational quanta of ϵ modes obtained from a modified valence force field investigation on Na_6MnS_4 using a QCPE program.[22,23,30] Magnetic field

(25) Vala, M. T.; Ballhausen, C. J.; Dingle, R.; Holt, S. L. *Mol. Phys.* **1972**, *23*, 217.
(26) Lever, A. B. P. *Inorganic Electronic Spectroscopy*, 2nd ed.; Elsevier: Amsterdam, 1984.
(27) Sinha, S. P.; Schmidtke, H.-H. *Mol. Phys.* **1965**, *10*, 7.
(28) Schmidtke, H.-H.; Adamsky, H.; Schönherr, T. *Bull. Chem. Soc. Jpn.* **1988**, *61*, 59.
(29) Dang Dinh Thong; Heimbrodt, W.; Hommel, D.; Goede, O. *Phys. Status Solidi A* **1984**, *81*, 695.

Table 2. Evaluated Lifetimes (μs) for the Three Components of Eq 1 from the Luminescence Decay at 12 K Obtained by Excitation at $\lambda_{exc} = 488$ nm

compound	red emission			yellow emission		
	τ_1	τ_2	τ_3	τ_1	τ_2	τ_3
Na_6MnS_4	124.5(3.0)	33.2(1.5)	6.7(0.8)	927.0(18)	268.0(10)	63.0(4)
K_2MnS_2	115.4(2.0)	29.5(1.1)	5.8(1.0)			
$Cs_2(Mn_{0.02}Zn_{0.98})_3S_4$	116.0(1.5)	34.8(1.6)	6.9(0.5)	1021.0(15)	660.0(12)	112.7(3)
$Cs_2(Mn_{0.08}Zn_{0.92})_3S_4$	114.9(3.0)	57.1(2.8)	*a*	*a*	*a*	*a*
$Cs_2Mn_3S_4$	52.7(4.5)	22.7(3.5)	5.0(1.5)			

[a] No evaluation possible due to low emission intensity.

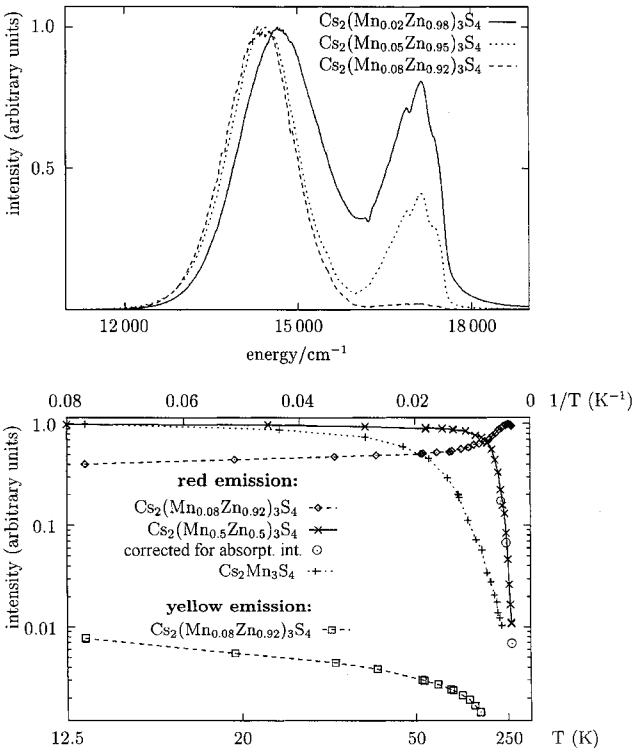

Figure 5. Emission spectra of $Cs_2(Mn_xZn_{1-x})_3S_4$ from crystal powders and different doping x at 13 K ($\lambda_{exc} = 488$ nm). Temperature dependence of the integral intensity of the red and yellow emission bands.

effects on excitation spectra of ZnS:Mn, however, suggest only a moderate $^4T_2 \times \epsilon$ coupling.[31] The fine structure can be as well due to a superposition of several vibrational modes. Notice also the distinct shift of the red emission peak by about 800 cm^{-1} toward lower energy when increasing the Mn concentration from $x = 0.02$ to 1.0, which we shall deal with further below.

3.3. Lifetimes. The decay data measured from the red and yellow luminescence of Na_6MnS_4 and the layer compounds with small Mn concentration ($x = 0.02$) do not follow simple exponential functions. A statistical evaluation using residuals, autocorrelation, and other criteria[3] for testing a fit to a hypothetical intensity decay formula supplies for both types of emissions a three-component function as

$$I(t) = \sum_{i=1}^{3} A_i e^{-t/\tau_i} \qquad (1)$$

More exponentials do not contribute to the quality of the adaptation which is limited by the number of measured data points. Also for the ZnS:Mn system a triexponential decay law has been reported.[33] A decay formula derived from energy transfer processes of molecular dipoles (Förster−Dexter mechanism[34]) had to be rejected due to passing of bounds imposed on the statistical test functions.[32] The time constants obtained by fitting the data points to the decay formula, eq 1, are compiled in Table 2. A dependence of the parameters, i.e., amplitudes A_i and lifetimes τ_i, on the detection wavelength could not be observed when using present experimental facilities. Simulation of emission decay by three exponential components indicates the presence of mainly three different sites with important concentrations in the crystals the origin of which cannot be identified. Contributions from higher closely lying energy level components belonging to the same multiplets can be excluded due to fast relaxations expected since the energy is bridged by crystal vibrational quanta which keep the nuclear framework unchanged.

Table 3. Temperature Dependence of Measured Lifetimes (μs)

	Na_6MnS_4							K_2MnS_2		
	red			yellow				red		
T (K)	$\tau_{1'}$	τ_1	τ_2	τ_1	τ_2	τ_3	T (K)	τ_1	τ_2	τ_3
12	*a*	124.5	33.2	927.0	268.0	63.0	12	115.4	29.5	5.8
23[b]	2707.1	149.0	35.4	925.8	165.1	50.9	22	91.8	24.2	4.3
45	2704.2	140.0	29.8	660.4	57.0	2.2	41	74.0	20.4	4.1
60	2686.8	121.3	28.5	369.1	38.5	*c*	60	71.4	22.7	3.8

[a] A lifetime corresponding to $\tau_{1'}$ is not detected; instead, a component $\tau_3 = 6.7$ μs (cf. Table 2) is observed. [b] Lifetime plots between 12 and 23 K exhibit a more elaborate time function than that of three exponentials. [c] Not to be evaluated due to low intensity.

Temperature dependent measurements of the red luminescence are presented in Table 3. The red emission of Na_6MnS_4 and of compounds with minor Mn concentration exhibits for temperature higher than 23 K a long-living component ($\tau_1 \rightarrow \tau_{1'}$). This observation which apparently is common to all compounds which show yellow and red luminescence simultaneously strongly supports an assignment of both emissions to MnS_4 molecular entities (see next section). Between 12 and 23 K the decay curve is more complicated than applying a fit by three exponentials as in eq 1.

(30) McIntosh, P. F.; Peterson, M. R. QCPE program No. 342, Chemistry Department, Indiana University, revised by Müller, A.; Eifert, K., Institut für Theoretische Chemie, Universität Düsseldorf.
(31) Parrot, R.; Boulanger, D.; Pohl, U. W.; Litzenburger, B.; Gumlich, H.-E. *Phys. Status Solidi B* **1998**, *207*, 113.
(32) Biertümpel, I.; Schmidtke, H.-H. *Chem. Phys.* **1997**, *215*, 271.
(33) Busse, W.; Gumlich, H.-E.; Meissner, B.; Theis, D. *J. Lumin.* **1976**, *12/13*, 693.
(34) Hennig, H.; Rehorek, D. *Photochemische und photokatalytische Reaktionen von Koordinationsverbindungen*; Teubner: Stuttgart, 1988.

Table 4. Parameters s (s^{-1}) and ΔE (cm^{-1}) of Eq 2 Evaluated from Temperature Dependent Lifetime Measurements

		red emission			yellow emission		
compound	i	τ_{i0}^{-1}	s	ΔE	τ_{i0}^{-1}	s	ΔE
Na_6MnS_4	1	3.7×10^2	1.4×10^7	1011(20)	1.1×10^3	1.5×10^2	112(5)
	2	6.7×10^3	4.0×10^6	560(25)	3.7×10^3	7.6×10^4	54(4)
	3	3.0×10^4	2.1×10^7	540(32)	1.6×10^4	1.1×10^5	54(5)
$Cs_2(Mn_{0.02}Zn_{0.98})_3S_4$	1	2.2×10^3	4.2×10^3	474(20)	1.0×10^3	8.9×10^2	153(8)
	2	8.7×10^3	4.5×10^4	469(20)	1.8×10^3	4.8×10^3	170(8)
$Cs_2(Mn_{0.08}Zn_{0.92})_3S_4$	1	8.8×10^3	6.9×10^5	403(25)	*a*	*a*	*a*
	2	1.8×10^4	1.3×10^5	439(30)	*a*	*a*	*a*

		red emission				
compound	i	τ_{i0}^{-1}	s_a	ΔE_a	s_b	ΔE_b
K_2MnS_2	1	8.6×10^3	3.7×10^5	466(25)	1.1×10^4	26(1)
	2	3.1×10^4	7.0×10^6	416(25)	3.4×10^4	18(1)
	3	1.7×10^5	3.0×10^7	419(30)	1.5×10^5	18(1)

[a] No definite evaluation possible due to low emission intensity.

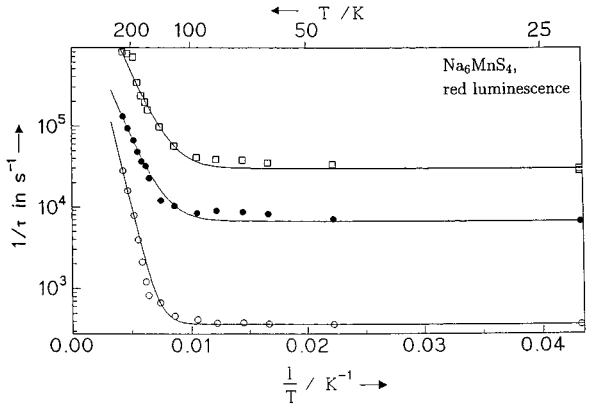

Figure 6. Arrhenius plot of the measured lifetimes depending on temperature for the red emissions. The solid curves mark the calculated functions obtained from the A_i, τ_i parameter fit.

Since luminescence from all compounds can be detected also at relatively high temperatures, the lifetime changes can be investigated within large temperature intervals. Arrhenius plots ($\ln(1/\tau)$ versus $1/T$) of the three measured lifetime components are illustrated in the case of the red emission of Na_6MnS_4 in Figure 6. Since the absorption intensity of systems with separate complex units changes only very little with temperature, a correction of emission has been neglected when determining lifetimes from eq 1. In the region between 23 and 80 K the τ_i parameters belonging to red luminescence do not vary very much with temperature. The yellow emission of Na_6MnS_4 exhibits larger temperature changes of τ_i starting already from 15 K on. Also all other compounds show a drastic decrease of lifetimes of red and yellow (if observable) emission at higher temperature.[22] The red emission lifetimes of K_2MnS_2 also decrease starting from 15 to 20 K but vary much slower with increasing temperature compared to the yellow emission in cases where both of these emissions are observed.

A fit of the measured lifetimes to the temperature function

$$\frac{1}{\tau_i} = \frac{1}{\tau_{i0}} + s_i e^{-\Delta E_i/kT} \quad \text{for} \quad i = 1, 2, 3 \qquad (2)$$

applying the common iterative least-squares procedure leads to activation energies, which are compiled in Table 4. The temperature independent term supplies the decay constant τ_{i0} at temperatures $T \rightarrow 0$. For a satisfactory fit of the K_2MnS_2 plots, two exponential terms are necessary, suggesting deactivation through more than one process. At low temperature the channel attributed to the smaller activation energy is the predominant component. Due to the instrumental difficulties arising from measuring the temperature directly on the sample, the activation energies are subject to errors of 5%. Note that the larger activation energies of K_2MnS_2 from the two measured are remarkably equal to those for corresponding emissions of the other compounds. Only the ΔE parameters of the mononuclear Mn complex ion are somewhat higher, which may result from the site symmetry, i.e., C_{3v}, for the mononuclear complex different from C_2 and D_2 for complexes with extended structures, the latter systems exhibiting very similar energy changes on molecular distortion as has been estimated from ligand field calculations.[19] The activation energies of the red and yellow emission presently obtained compare well with $\Delta E^{red} = 450\ cm^{-1}$ and $\Delta E^{yellow} = 170\ cm^{-1}$ reported for different Mn concentration doped in ZnS.[11,12,29]

4. Model for Explaining the Luminescence Properties

Summarizing the above findings we will come to the conclusion that both the yellow and the red emissions result from electronic levels primarily due to d electrons of isolated Mn complex entities which are subject to a minor interaction with their neighbors. This follows from magnetic properties which closely obey the Curie−Weiss law[18,20,21]and is well-supported by the spectroscopical results presented in the preceding sections.

The absorption spectra of isolated complexes, of complex chains, and of layers can be explained on the basis of the AOM, applied on a local mononuclear species, which is able to simulate the excited d-level energies very well (as we have seen in section 3.1). All compounds, i.e., those emitting exclusively red and those exhibiting both red *and* yellow emission, show remarkably similar absorption and excitation spectra as is illustrated by the equal numbering of spectral peaks (cf. Figures 1−3) indicating closely related energy level systems. Also the temperature dependence of lifetimes is very similar (section 3.3). Red emission, which in the

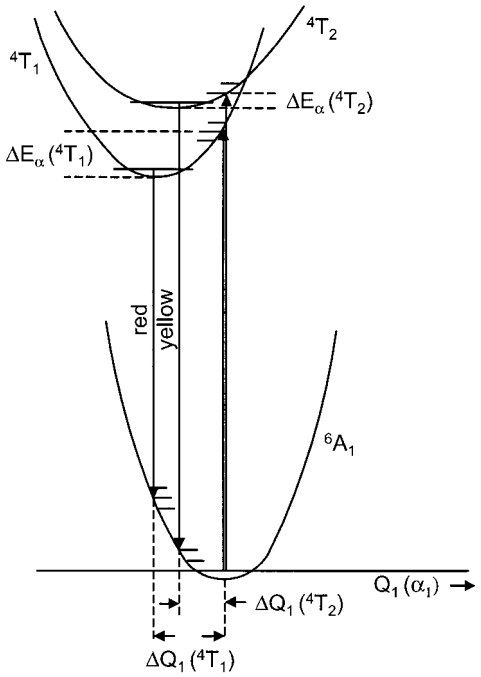

Figure 7. Potential curves of ligand field levels for a MnS_4 cluster (schematic) providing a model explaining the observed emission properties. A similar plot will be obtained for an appropriate projection in the Q_2, $Q_3(\epsilon)$ space (see text).

literature has been generally attributed to cooperative effects between different Mn complex units or special "red centers",[3−5,11−13] is observed as well from systems of isolated Mn complexes, as in Na_6MnS_4 and $Cs_2(Mn_xZn_{1-x})_3S_4$ of low Mn concentration, and is similar to that observed for complexes with extended structures, i.e., K_2MnS_2 and Cs_2-Mn_3S_4 (section 3.2). In addition, a complex with dithioimidodiphosphinate ligands which largely separate the emitting Mn centers also exhibits red luminescence.[24,35] As outlined in section 3.3 the luminescence decay can only be simulated by exponential time functions and not, e.g., by decay formulas derived from a model of interacting molecular dipoles. Similar activation energies of the red emission obtained for the chain compound and the isolated species in the slightly doped materials (cf. Table 4) indicate equal energy transfer mechanisms confirming local energy levels for these systems.

The transitions between $^4T_1$ and $^4T_2$ to the $^6A_1$ ground state are spin forbidden; one is symmetry allowed in T_d symmetry by electric dipole transitions, the other vibronically allowed involving ϵ or τ_2 vibrational modes. Intensity is obtained through level mixing of excited quartets and the sextet ground state by spin−orbit coupling and by virtue of lower symmetry in the crystals providing level splittings.

The main features obtained from the emission measurements can be explained by a system of potential energy curves for the MnS_4 complex as it is illustrated schematically in Figure 7. The levels are classified in tetrahedral notation neglecting spin−orbit coupling which is justified since further distortion, e.g., C_{3v} as reported for Na_6MnS_4,[21] and spin−orbit splittings are small. The potential curves are shown with respect to the totally symmetric coordinate $Q_1(\alpha_1)$ since symmetrical stretching vibrations mainly contribute to vibronic coupling causing the main shift of potential minima compared to the ground state.[36,37] This shift is expected toward smaller atomic distances since the excited ^4T levels result predominantly from the electron configuration $e^3t_2^2$ with fewer d electrons in partially σ-antibonding t_2 than in the $^6A_1$ ground state which arises from $e^2t_2^3$ ($e < t_2$ in energy and antibonding strength). The Mn−S bonds are therefore expected to be stronger in the excited states, and the force constants are increased compared to the ground state. The shift of the lower excited $^4T_1$ level is somewhat larger than for $^4T_2$, as is indicated in Figure 7, because configuration interaction (CI) supplies intermixing with higher quartet levels providing similar antibonding effects as in $^6A_1$, a process which is larger for $^4T_2$ than for $^4T_1$.[19,22] A calculation of vibronic coupling for tetrahedral coordination,[38] performed with the ligand field parameters given in Table 1 and applying the force constants F_{11} obtained from a modified valence force field investigation, furnishes potential energy shifts $\Delta Q_1(\alpha_1) = -4.3$ and -2.1 pm and stabilization energies $\Delta E_1(\alpha_1) = -85$ and -20 cm^{-1} for $^4T_1$ and $^4T_2$, respectively.[22,23]

Since the yellow emission spectra of compounds with separate MnS_4 units show indications for a progression in ϵ modes [22,23,38] (cf. Figure 5), we also considered vibronic coupling of $^4T_1$ and $^4T_2$ with ϵ vibrations and calculated corresponding potential energy curves as those in the Q_1-(α_1) space: both excited state curves are shifted to smaller Mn−S atomic distances compared to the ground state; the shift of the $^4T_1$ is, however, smaller than that of $^4T_2$. A figure very similar to Figure 7 can be drawn if in the three-dimensional plot $E(Q_2,Q_3)$ is projected on a plane going through one of the three equivalent minima of T orbital components.[39]

A corresponding calculation (neglecting CI) of vibronic coupling for $T_1 \times \epsilon$ coupling furnishes $\Delta E_{2,3}(\epsilon) = -57$ cm^{-1} and $\Delta Q_{2,3}(\epsilon) = -4.29$ pm (inclusion of CI reduces somewhat the absolute value of both of these data; for numerical values the calculation would need the parameter η[36,38] not available from the present experiment) which is of an order similar to that of the results obtained for α coupling. Although the ΔQ value gives a change of valence angles of only $\alpha = 0.5°$, potential energies in the ϵ space should be considered simultaneously with the distortions in the α_1 space. This would, however, complicate the present model drastically with a loss of insight into the vibronic coupling mechanism. The discussion which follows, therefore, will be carried out using a plot as Figure 7 which either applies for the $Q_1(\alpha_1)$ coordinate as indicated or applies as a projection in the Q_2, $Q_3(\epsilon)$ space.

(35) Siiman, O.; Wrighton, M.; Gray, H. B. *J. Coord. Chem.* **1972**, *2*, 159.
(36) Schmidtke, H.-H.; Degen, J. *Struct. Bonding* **1989**, *71*, 100.
(37) Denning, R. G. In *Vibronic Processes in Inorganic Chemistry*; Flint, C. D., Ed.; NATO Advanced Science Institute Series C: Kluwer Academic Publishers: Dordrecht, 1989; Vol. 288.
(38) Wissing, K.; Degen, J. *Mol. Phys.* **1998**, *95*, 51.
(39) Englman, R. *Jahn−Teller Effect in Molecules and Crystals*; Wiley Interscience: New York, 1972.

The red emission, which is observed for all compounds, is the standard emission from the lowest excited state $^4T_1$ following Kasha's rule.[40] The yellow emission detected in Na_6MnS_4 and weakly doped layer compounds, on the other hand, results from the higher $^4T_2$ level. Irradiation by continuous laser excitation ($\lambda_{exc} = 488$ nm) occupies higher vibrational levels of $^4T_1$ and $^4T_2$ followed by fast relaxation through channels into their zero-phonon levels. If the activation barrier between these states allows, energy exchange from the "yellow level" to the "red level" may occur at low temperature. In any case red *and* yellow emission is observed. Excitation with light of higher frequency keeping the other parameters constant is found to supply more yellow compared to red emission. At temperature higher than about 23 K for compounds containing separate MnS_4 complexes, another species appears which exhibits a long-living red emission (see Table 3) that is not observed at lower temperatures ($A_{1'} = 0$). This may be attributed to unique MnS_4 entities employing smaller interaction with the environment than those in extended structures. Apparently the geometry of this species has a symmetry closer to T_d in which $^4T_1 \rightarrow {}^6A_1$ transitions are symmetry-forbidden (in addition to spin-forbidden), making electric dipole transitions less probable. Promotion of red emission intensity connected with decreased yellow emission is generally observed when increasing the power of the excitation light which obviously is due to a heating of the sample. This observation is reversible: power reduction of excitation light favors yellow emission compared to red emission. For compounds such as K_2MnS_4 and $Cs_2Mn_3S_4$ forming extended molecular structures, we can assume more effective energy exchange between the two deactivation channels through $^4T_1$ and $^4T_2$ vibronic levels as well as population of "red levels" from the "yellow levels" giving rise to only red emission. The highly doped $Cs_2(Mn_xZn_{1-x})_3S_4$ systems follow this mechanism as well: increased interaction (or clustering) between complexes for larger Mn concentration leads to improved $^4T_2-{}^4T_1$ level exchange such that excitation energy will be collected in the lower quartet level providing merely red emission. The reason for this higher level mixing is attributed to stronger cooperative effects which decrease the molecular symmetry more effectively to lower than cubic. This view is supported by a lowering of the activation energy for systems of higher Mn concentration which favors the energy transfer promoting the red emission (see Table 4). A model of increasing level dispersions and smaller energy gaps with larger Mn clustering can also explain the observed shift of the red emission toward lower energy (cf. Figure 5).

The temperature-dependent measurements are also in agreement with the present model. The activation energies are in all cases lower for the Mn yellow luminescence than for the red luminescence. For Na_6MnS_4 they are 50−110 cm^{-1} (Table 4), which is on the other hand too large for completely depopulating the $^4T_2$ level by relaxation into $^4T_1$ at low temperature such that yellow emission over red emission is favored (see Figure 4). The crossing of the two emission intensity curves is well within the temperature range in which the drastic lifetime change of red emission is observed (Table 3). The constant red emission intensity increasing even in the temperature range >23 K, where the long-living emission is detected, results from the high population of the $^4T_1$ state provided by the particular design of activation channels and feeding from "yellow" levels.

The potential curves depicted in Figure 7 may be used for discussing the bandwidths of yellow and red emission as well. Since the red luminescence originates from a potential curve $^4T_1$ which in $Q_1(\alpha_1)$ space is more shifted with respect to the ground state than the curve of the next higher excited state $^4T_2$, the transition arrives at a steeper descent of the ground state than the yellow emission, giving rise to an excitation of a larger number of vibrational quanta, which results in a broadening of the emission band. In the corresponding plot of Q_2, $Q_3(\epsilon)$ space the $^4T_2$ curve is more shifted than the $^4T_1$ curve, which would result in a broader emission band for the yellow emission compared to the red emission. Since bands in Figures 4 and 5 are evidently narrower for yellow emissions, the plot in $Q_1(\alpha_1)$ space would be more appropriate for explaining the observed luminescence.

5. Conclusions

The red emission of tetrahedrally coordinated Mn(II) observed from systems as different as ZnS:Mn,[1−8] Mn(ph_4-dithioimidodiphosphinato)$_2$,[24,35] and all present thiomanganate compounds with various types of structures is conveniently attributed to MnS_4 complex levels following Kasha's rule.[40] Since systems containing separate MnS_4units, such as ZnS:Mn, Na_6MnS_4, and $Cs_2(Mn_xZn_{1-x})_3S_4$ with low Mn concentration, exhibit yellow *and* red emission as well, earlier explanations by charge transfer transitions between clusters or by particular red centers equally present in all these systems are hardly satisfactory. An assignment of both the red and yellow emission to MnS_4 chromophores in all compounds is supported by results from lifetime and activation energy measurements which can be obtained over a large temperature range. A model of potential energy plots of the two lowest excited electronic levels in tetrahedral coordination can rationalize the experimental results.

Acknowledgment. The authors are grateful to Prof. Dr. W. Bronger and Dr. M. Kanert from the Rheinisch-Westfälische Technische Hochschule Aachen, Germany, for supplying us with the Mn complexes. We also thank Dr. I. Biertümpel, Prof. Dr. J. Degen, and Dr. K. Wissing from the present institute for several interesting discussions and Mr. R. Linder for experimental assistance.

IC010333C

(40) Kasha, M. *Discuss. Faraday Soc.* **1950**, *9*, 14.